

ICE AGE GEODYNAMICS

✱ 10149

W. R. Peltier

Department of Physics, University of Toronto, Toronto, Ontario, Canada, M5S 1A7

INTRODUCTION

The study of glacial isostasy is concerned with the interpretation of that set of geophysical observables unambiguously associated with the response of the Earth to the massive continental deglaciations that marked the end of the last glacial epoch of the current ice age. These globally synchronous deglaciations, which began ca 18 KBP (thousands of years before present), resulted in the addition to the oceans of approximately 10^{19} kgm of water (see, for example, Peltier & Andrews 1976), which effected a mean global rise of sea level on the order of 80 meters. The major ice sheets that served as the source of this meltwater were the Laurentide-Innuitian complex of North America and the Fennoscandian complex of North Western Europe. On the basis of time series of the relative abundances of the isotopes O^{16} and O^{18} , obtained from deep sea sedimentary cores (see, for example, Broecker & van Donk 1970), from which one may infer the extent of northern hemisphere continental ice coverage, we know that the major ice sheets had existed on the surface for roughly 10^5 years prior to their disintegration, a time scale over which they were slowly, if not monotonically, approaching their maximum extents (Andrews & Barry 1978). Because of the enormous scale of these glacial complexes they exerted considerable mechanical stress on the underlying planet by virtue of their mutual gravitational attraction. It is fortunate for the subject of geodynamics that the planet has conspired to "remember" its response to this applied stress and it is for this reason that Reginald Daley (1934) was led to refer to the deglaciation event itself as "nature's great experiment."

The importance of this experiment is that, through interpretation of the data it produced, we may directly investigate the nature of the rheological law governing the long timescale response of mantle material to an applied stress. Such information is a crucial ingredient required in the construction of thermal convection models for plate tectonics (Peltier



Figure 1 Photograph of a flight of raised beaches in the Richmond Gulf of Hudson Bay near the center of rebound. Photo courtesy of Professor C. Hilaire-Marcel.

1980b). A second type of information that may also be extracted through interpretation of the results of this natural experiment concerns the detailed history of the melting event itself and this is important in understanding the mechanism of climatic change.

The main observational data that we are interested in explaining consist of histories of relative sea level obtained by the C^{14} dating of marine shells or other in situ carbonaceous material from relict beaches found either above or below present-day sea level. The photograph shown in *Figure 1* is of a flight of raised beaches found in the Richmond Gulf of Hudson Bay, near what was the center of the ancient Laurentide ice sheet. When the height above present-day sea level of each of the beach horizons is plotted as a function of isotopic age (corrected to give proper sidereal age) then one obtains the relaxation curve shown in *Figure 2* in which the oldest beach is found at the greatest height above m.s.l. (mean sea level). These data show that the surface of the solid earth at this site has been continuously elevated above the geoid since the removal of the ice load and that the rate of this uplift has been an exponentially decreasing function of time.

Complementing such pointwise relaxation data and providing (as we shall see) an equally important key to the rheological puzzle, are maps of

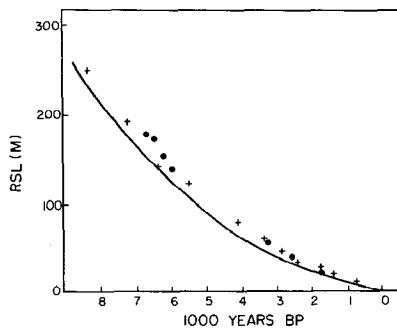


Figure 2 Relaxation curve based upon C^{14} dates of the beaches in Richmond Gulf compared with a theoretical prediction using the ICE-3 deglaciation history (to be discussed in a later section) and an Earth model with constant mantle viscosity. Figure is from Peltier (1980).

the present-day free-air gravity anomaly over the once ice-covered regions. Free-air anomaly data for Fennoscandia are discussed in Balling (1980), for example, and reveal a maximum negative anomaly over the once ice-covered region of between 15 and 20 milligals. An equivalent map for the Laurentide region was compiled by Walcott (1970) and is discussed in some detail later in this article. Here the maximum observed negative anomaly is on the order of 35 milligals.

That the sea level and gravity data do contain important rheological information should be immediately clear. Since the melting of the ice sheets was certainly complete by 5 KBP and most probably by 6.5 KBP (Prest 1969), relaxation data such as those shown in Figure 2 conclusively establish that the Earth cannot be described as a Hooke's Law solid. If it could be so described then the quasi-static deformation forced by the shifting surface load would have ceased with the cessation of melting. Even though the Hookean rheology is universally agreed to provide a reasonable description of short timescale seismic processes, it is completely inadequate insofar as the understanding of postglacial rebound is concerned. Even in the seismic regime, however, anelastic processes are important and produce observable effects, such as the dispersion of body wave velocities (Liu et al 1976), and endow the elastic gravitational free oscillations with finite Q (see, for example, Buland & Gilbert 1978). Such high frequency anelasticity is apparently well described by a linear viscoelastic absorption-band model (Anderson & Minster 1979, Minster 1980), which is capable of delivering the weak dependence of intrinsic Q upon frequency observed in the seismic regime. Such a model, however, does not allow steady-state creep so that if it were a complete representation of mantle rheology then thermal convection would be impossible and

continental drift an indefensible hypothesis. That this is in fact the case is a view still held by a minority of Earth scientists (e.g. Jeffreys 1973).

More likely, however, is the possibility that the transient creep of the absorption-band model is followed by steady-state deformation and this is in accord with laboratory observations of the creep of Olivine single crystals (Kohlstedt & Goëtze 1974). It is presumably such steady-state creep that governs both postglacial rebound and mantle convection (Peltier et al 1980a). A linear viscoelastic approximation to the complete rheology must then consist of an absorption-band model (i.e. a standard linear solid with a continuous spectrum of relaxation times) in series with a Maxwell element to give a modified Burgers body solid (Peltier et al 1980b). In the long time limit such a solid behaves as a Newtonian viscous fluid, which is characterized by a linear relation between stress and strain rate. Laboratory data suggest that this might only be an approximation since they show, in the high creep rate regime where the experiments must be performed, that the stress-strain relation is nonlinear. It is still unclear whether or not at relevant mantle strain rates the deformation mechanism might be Newtonian but recent analyses (Twiss 1976) suggestive of structural superplasticity conclude that this could well be the case.

In total (and perhaps blessed!) ignorance of these microphysical complexities, early attempts to interpret the relaxation data from glacial isostasy were based almost exclusively upon the assumption that the Earth behaved entirely as a Newtonian viscous fluid insofar as the long timescale adjustment phenomenon was concerned. A rather complete account of the major achievements of interpretation up to and including the year 1973 will be found in the review by Walcott (1973). In Walcott's view the preferred model for the mantle viscosity profile based upon this work consisted of "a 110 km thick lithosphere which, although requiring a viscosity of 10^{25} P[oise] to explain some long-term behavior, behaves elastically on time scales of a few thousand years; a thin, low viscosity channel some 100–500 km thick with a viscosity dependent upon thickness of 10^{19} to 10^{21} P[oise]; and a lower mantle viscosity greater than 10^{24} P[oise]." In Walcott's opinion the totality of the evidence then available tended to support the previously stated conclusions of McConnell (1968) and others to the effect that the viscosity of the lower mantle was significantly in excess (by at least two orders of magnitude) of the viscosity of the upper mantle. He considered the lower mantle value of 10^{24} Poise to be a *lower* bound upon the actual value, which he believed could be very much higher.

The question of the viscosity of the lower mantle relative to that of the upper mantle is an extremely important one insofar as models of mantle convection are concerned. The simple geometric argument given in Peltier

(1973), for example, suggests that for a mantle of uniform chemical composition an increase of viscosity by more than two orders of magnitude across the 670 km seismic discontinuity would be required to focus a distinct circulation into the upper mantle region. Otherwise, whole mantle convection would be preferred (Peltier 1973, 1980b, Sharpe & Peltier 1978, 1979) with a single cellular motion in the radial direction having a vertical extent comparable to the mantle thickness. The view expressed by Walcott in 1973 was necessarily conditioned by extant models of the rebound process. These models were deficient in several important respects and since that time a more complete and internally self-consistent theory of postglacial rebound has become available, in terms of which a more accurate description of the phenomenon is possible. In the following sections, the main ingredients of this new theory are reviewed and the revision of our notion of the mantle viscosity profile, which the new analyses require, is assessed.

THE THEORY OF GLACIAL ISOSTASY

The physical basis of the new model of isostatic adjustment is embodied in a mechanical constitutive relation that provides a macroscopic connection between stress and strain. Insofar as the long timescale rebound process is concerned, we shall assume that the mantle may be described as a linear viscoelastic Maxwell solid for which the stress tensor τ_{ij} and the strain tensor e_{ij} are related as (Peltier 1974)

$$\dot{\tau}_{ij} + \frac{\mu}{\nu} (\tau_{ij} - \frac{1}{3}\tau_{kk}\delta_{ij}) = 2\mu\dot{e}_{ij} + \lambda\dot{e}_{kk}\delta_{ij}, \quad (1)$$

where the dot denotes time differentiation, μ and λ are the conventional Lamé parameters of Hookean elasticity, and ν is the molecular viscosity. In the Laplace transform domain of the imaginary frequency s , (1) takes the form

$$\tilde{\tau}_{ij} = \lambda(s)\tilde{e}_{kk}\delta_{ij} + 2\mu(s)\tilde{e}_{ij} \quad (2)$$

where the tilde indicates implicit dependence upon s , and where $\lambda(s)$ and $\mu(s)$ are the compliances

$$\lambda(s) = \frac{\lambda s + \mu K/\nu}{s + \mu/\nu}; \quad \mu(s) = \frac{\mu s}{s + \mu/\nu}, \quad (3)$$

where $K = \lambda + 2\mu/3$ is the elastic bulk modulus. When it is subject to an applied stress, the Maxwell solid exhibits an initial response which is

Hookean elastic. As time proceeds, however, the behavior tends asymptotically to that of a Newtonian fluid for which the deviatoric stress depends linearly upon the strain rate. Inspection of the Laplace transform domain compliances (3) shows that the time scale over which this transition in behavior is achieved is the Maxwell time $T_m = \nu/\mu$. In the upper mantle, where the viscosity is on the order of 10^{22} Poise, the elastic shear modulus is such that $T_m \simeq 200$ years. One of the ideas we hope to test by fitting the Maxwell model to the postglacial rebound data is whether the radial profile $v(r)$ that we obtain is acceptable from the point of view of models of the mantle convection process. It is important to note that, although the Maxwell model is in itself an incomplete description of mantle rheology, the missing short timescale anelasticity required to understand seismic Q does not affect the inference of $v(r)$ (Peltier et al 1980b).

Because the strains produced by ice sheet and ocean loading are sufficiently small, the deformation history may be described in terms of the Laplace transformed and linearized field equations for the conservation of momentum and for the gravitational field. These are respectively

$$\nabla \cdot \tilde{\tau} - \nabla(\rho g \mathbf{u} \cdot \mathbf{e}_r) - \rho \nabla \phi + g \nabla \cdot (\rho \tilde{\mathbf{u}}) \mathbf{e}_r = 0, \quad (4a)$$

$$\nabla^2 \tilde{\Phi} = -4\pi G \nabla \cdot (\rho \tilde{\mathbf{u}}), \quad (4b)$$

where $\rho = \rho(r)$ is the density field in the background (undeformed) hydrostatic and spherical equilibrium configuration, $g = g(r)$ is the corresponding gravitational acceleration, \mathbf{u} is the displacement field, \mathbf{e}_r is a unit vector in the radial direction, ϕ is the perturbation of the ambient gravitational potential associated with the deformation, and G is the gravitational constant. The inertial force in (4a) is suppressed because of the long time scale of the adjustment process.

The essential purpose of the theory is to employ (4) to determine the response of the Earth to the space- and time-dependent ice and water loads applied on its surface. We proceed first to calculate the response of the planet to impulsive loading by a point mass and thus to construct a Green's function for the gravitational interaction problem. We may then invoke the principle of superposition to describe the response to a realistic loading history.

If in its unperturbed state the Earth may be well approximated as a radially stratified sphere, then the response to a point mass load on its surface will be a function only of radius r , angular distance from the applied load θ , and time t . The solution three vector (\mathbf{u}, ϕ) to equations (4) may then be expanded in vector spherical harmonics as

$$\tilde{\mathbf{u}} = \sum_{n=0}^{\infty} (U_n(r, s) P_n(\cos \theta) \mathbf{e}_r + V_n(r, s) \frac{\partial P_n}{\partial \theta}(\cos \theta) \mathbf{e}_\theta), \quad (5a)$$

$$\tilde{\phi} = \sum_{n=0}^{\infty} \Phi_n(r, s) P_n(\cos \theta), \quad (5b)$$

where U_n , V_n , Φ_n are spectral amplitudes for the harmonic disturbances of degree n in radial and tangential displacement and in the perturbation to the ambient gravitational potential respectively. When (5) are substituted in (4) they reduce the field equations to a set of six coupled ordinary differential equations of the form

$$\frac{d\mathbf{Y}}{dr} = \mathcal{A}\mathbf{Y} \quad (6)$$

where $\mathbf{Y} = (U_n, V_n, T_{rn}, T_{\theta n}, \Phi_n, Q_n)$ and \mathcal{A} is a complicated 6×6 matrix of coupling coefficients given explicitly in Peltier (1974). T_{rn} and $T_{\theta n}$ are spectral amplitudes in the expansions for radial and tangential stress and Q_n are those in the expansion for the auxiliary variable $q = \partial\phi/\partial r + (n+1)\phi/r + 4\pi G\rho r$. To determine the response of the Earth to the point mass load we solve (6) subject to the following boundary conditions, which obtain at the Earth's surface $r = a$:

$$T_{rn} = -g(2n+1)/4\pi a^2, \quad (7a)$$

$$T_{\theta n} = 0, \quad (7b)$$

$$Q_n = -4\pi G(2n+1)/4\pi a^2, \quad (7c)$$

which follow respectively (Peltier 1974) from the condition that the normal stress balance the applied load, that the tangential stress vanish, and that the radial derivative of the potential possess the correct discontinuity to account for the surface density of the load.

Solutions of (6) subject to (7) are most economically expressed in terms of the triplet of dimensionless scalars called surface load Love numbers which are denoted by (h_n, l_n, k_n) and defined through

$$\begin{bmatrix} U_n(r, s) \\ V_n(r, s) \\ \Phi_n^1(r, s) \end{bmatrix} = \Phi_n^2(r) \begin{bmatrix} h_n(r, s)/g \\ l_n(r, s)/g \\ k_n(r, s) \end{bmatrix} \quad (8)$$

where the expansion $\Phi_n = \Phi_n^1 + \Phi_n^2$ has been employed, in which Φ_n^1 are the harmonic coefficients in the expansion for the field of force which produces U_n , V_n , Φ_n^1 in response. Φ_n^2 are independent of the Laplace transform variable because the surface point mass load is applied impulsively (i.e. as a Dirac delta function in the time domain).

In Figure 3 we show an example of the surface $h_n^V(a, s)$ for a realistic viscoelastic model of the Earth, which has an elastic lithosphere of thickness $T = 120$ km, a constant viscosity mantle with $\nu = 10^{22}$ Poise, and an

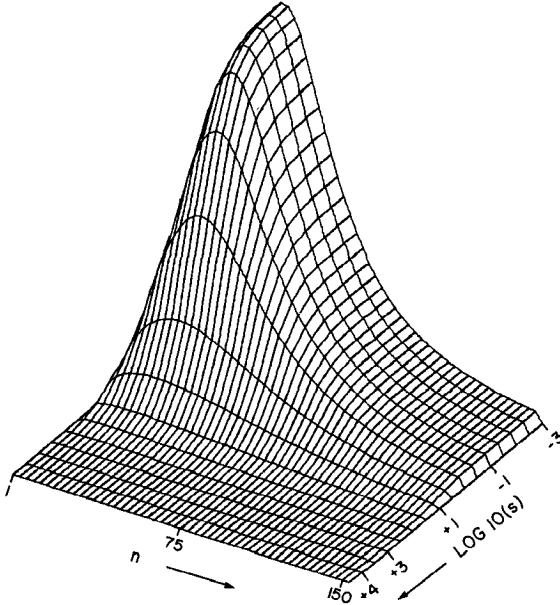


Figure 3 Three-dimensional view of the Laplace transform domain relaxation surface $h_n^V(s)$. Note that as $n \rightarrow \infty$, $h_n^V \rightarrow 0$ and the viscous relaxation is completely suppressed. Figure is from Peltier et al (1978).

inviscid core. The elastic structure of the model $[\rho(r), \lambda(r), \mu(r)]$ is that obtained from the inversion of elastic gravitational free oscillation data (Gilbert & Dziewonski 1975). The viscous part of the surface load Love number is just $h_n^V(a, s) = h_n(a, s) - h_n^E(a)$ where h_n^E is the Love number previously calculated by Farrell (1972) and others for the Hookean elastic rheology. Figure 3 shows that for short deformation wavelengths (large n), the viscous part of the response to the applied point mass load tends to zero, an affect that is due to the presence of the elastic lithosphere. Also evident from this figure is the existence of spectral asymptotes at both large and small values of s , which correspond via the Tauberian theorems to small and large values of time t respectively.

As shown in Peltier (1976), each spectrum $h_n(a, s)$ has an *exact* normal mode expansion of the form

$$h_n(a, s) = \sum_j \frac{r_j^n}{s + s_j^n} + h_n^E, \tag{9}$$

where the s_j^n are a set of poles on the negative real s -axis of the complex s -plane and where the r_j^n are the residues at these poles which measure the

Annu. Rev. Earth. Planet. Sci. 1981.9:199-225. Downloaded from arjournals.annualreviews.org by University of Toronto on 06/14/06. For personal use only.

extent to which each of the associated modes is excited by the point forcing. The relaxation times $\tau_n^j = 1/s_n^j$ associated with each of these modes may be computed by solving the associated homogeneous eigenvalue problem. Figure 4 shows such normal mode relaxation spectra for several different viscoelastic models of the planet. These models have been constructed to illustrate the individual components of the spectrum for a realistic Earth model, which is shown in plate *d*. The spectrum in plate *a* is for a homogeneous viscoelastic sphere, which has only one mode for each wavenumber n . This modal branch has relaxation time increasing with n such that for n large we have $s \approx g\rho/2\nu k_H$ which is the relaxation spectrum for a viscous halfspace (k_H is the horizontal wavenumber). Plate *b* shows the effect of adding a lithosphere to the otherwise homogeneous model and this is seen to introduce a second mode for each n and to force the relaxation time of the fundamental mode to *decrease* with increasing n for $n \gtrsim 30$. It was on the basis of his observation of this effect in the Fennoscandia data that McConnell (1968) was originally led to infer the existence of a lithosphere with a thickness of about 110 km. In plate *c* we

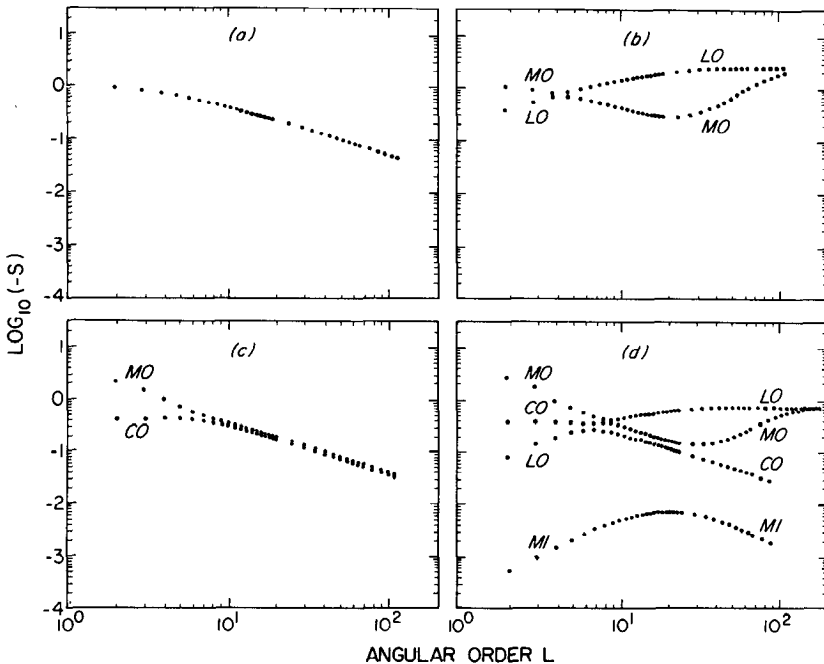


Figure 4 Relaxation diagrams for the four Earth models described in the text. The relaxation times $\tau_n = s_n^{-1}$ are plotted on a logarithmic scale and measured in units of 10^3 years. Figure is from Peltier (1980).

illustrate the effect of adding a high density inviscid core to the homogeneous model and note that this feature also introduces a second relaxation time for each n and that for this extra mode, as for the fundamental, relaxation time increases with n . Plate d is the spectrum for a complete Earth model which is seen to contain all of the individual features mentioned above plus additional modes which have particularly long relaxation times and which are due to the sharp increases of density in the transition zone associated with the Olivine-Spinel and the Spinel-post Spinel phase changes.

Since the Love number spectra have simple normal mode decompositions of the form (9) they possess trivial time domain representations

$$h_n(a, t) = \sum_j r_j^n e^{-s_j^n t} + h_n^E \delta(t), \quad (10)$$

which are the time domain spectral amplitudes for the impulsive point forcing. The r_j^n in (10) and (9) are determined by employing the known s_j^n as pivots in the collocation method discussed in Peltier (1976). If the point mass were allowed to remain on the surface for $t \geq 0$, then the coefficients for the resulting deformation may be obtained simply from (10) by convolution with a Heaviside step function. This operation yields (suppressing a)

$$\begin{aligned} h_n^H(t) &= \sum_j \frac{r_j^n}{s_j^n} (1 - e^{-s_j^n t}) + h_n^E \\ &= h_n^{H,V}(t) + h_n^E. \end{aligned} \quad (11)$$

Note that (9) and (11) are related by

$$\lim_{t \rightarrow \infty} h_n^H(t) = \sum_j \frac{r_j^n}{s_j^n} + h_n^E = \lim_{s \rightarrow 0} h_n(s), \quad (12)$$

which clearly reveals the isostatic compensation mechanism since the number $\sum_j r_j^n/s_j^n$ for each n is just the viscous contribution to the final isostatically adjusted amplitude and this is a unique number for all Earth models which differ from one another only through their mantle viscosity profiles (Peltier 1976, Wu & Peltier 1981a). Examples of $h_n^{H,V}(t)$ spectra are shown in Peltier et al (1978) for the realistic Earth model with constant mantle viscosity. For $n \gtrsim 150$ the viscous response vanishes and such short wavelength loads are supported elastically.

In order to describe the response of the planet to an arbitrary surface load that is variable in both space and time, we construct Green's functions for the inhomogeneous boundary value problem and invoke the principle of superposition. These Green's functions may be computed for various signatures of the response in terms of the Love numbers h_n , l_n , k_n . Here we shall concern ourselves only with those for radial displacement, gravity

anomaly, and the perturbation to the potential field, which have the respective representations (Peltier 1974):

$$u_r^H(\theta, t) = \frac{a}{m_e} \sum_{n=0}^{\infty} h_n^H(t) P_n(\cos \theta), \quad (13a)$$

$$\alpha^H(\theta, t) = \frac{g}{m_e} \sum_{n=0}^{\infty} [n - 2h_n^H(t) - (n + 1)k_n^H(t)] P_n(\cos \theta), \quad (13b)$$

$$\phi^H(\theta, t) = \frac{ag}{m_e} \sum_{n=0}^{\infty} [1 + k_n^H(t) - h_n^H(t)] P_n(\cos \theta). \quad (13c)$$

Depending upon the nature of the Earth model, the above infinite series may be slowly convergent and acceleration techniques such as the Euler transformation may be required to sum them (Peltier 1974). In Figure 5 the $u_r^{H,V}(\theta, t)$ Green's function is shown for the realistic Earth model with constant mantle viscosity. For plotting purposes the function has been normalized by multiplication with " $a\theta$ " to remove the geometric singularity at $\theta = 0$. Note that the θ scale is logarithmic. As may be seen by inspection of (11), the viscous part of the response vanishes at $t = 0$, then

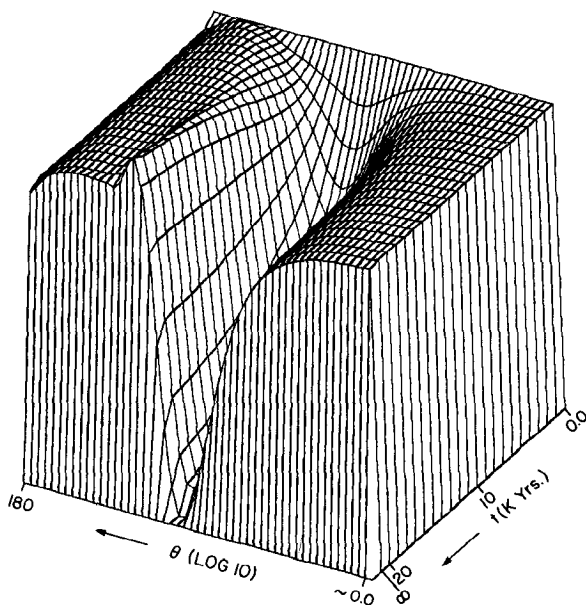


Figure 5 Viscous part of the Green's function for radial displacement for the Earth model whose relaxation spectrum is shown in plate (d) of Figure 4. The response has been normalized by multiplication with " $a\theta$ " to remove the effect of the geometric singularity at $\theta = 0$ for plotting purposes. Figure is from Peltier et al (1978).

increases with time as the surface sags under the applied load, eventually reaching the deformed equilibrium state in which isostatic (gravitational) equilibrium prevails. Note that in the region peripheral to the load the planetary radius increases above its equilibrium value to create a "peripheral bulge" surrounding the point mass. It is the collapse of this bulge, following removal of a compensated load, that explains the observed submergence in the immediately peripheral regions (Peltier 1974).

Given these response functions, we may next consider how they are to be employed to predict observations of the type described in the introduction. In order to make a prediction we require a priori information concerning the deglaciation history and this may be obtained with reasonable accuracy in the manner described in Peltier & Andrews (1976). Inspection of relative sea level variations (drowned beaches) in the far field of the ice sheets provides an estimate of the amount of water that was added to the ocean basins as a function of time during melting. Knowing the location of the ice sheet margins as a function of time from end moraine data, the water load is simply partitioned back to the ice sheets in the ratio of their instantaneous areas. Ice mechanical arguments (Patterson 1972) allow us to obtain an approximation to the instantaneous topography. On the basis of such information, Peltier & Andrews (1976) produced approximate disintegration histories for the major ice sheets. In Figure 6a-f we show a sequence of time slices through their disintegration histories for both the Laurentide-Innuitian complex and for Fennoscandia (this model will be referred to subsequently as ICE-1). It should be emphasized that these reconstructions are to be viewed as first approximations, which will undoubtedly require modification to correct certain characteristic misfits between observation and theoretical prediction. It is a characteristic feature of the problem of glacial isostasy that its solution involves the determination of two unknown functionals of the theoretical model. Neither the deglaciation history nor the viscosity profile are known perfectly in advance and so the inverse problem for either is intrinsically nonlinear.

If there were a set of geophysical data that provided an accurate memory of the change in local radius of the planet produced by ice sheet disintegration, then we could make a theoretical prediction to compare with the observation simply by convolving the radial displacement Green's function (13a) with the surface load history to give

$$\Delta R(\theta, \phi, t) = \iint d\Omega' \int u_r(\theta|\theta', \lambda|\lambda', t|t') M(\theta', \lambda', t') dt', \quad (14)$$

where M is the (assumed known) load history. Notwithstanding the fact that there is *no* geophysical data that provides a direct memory of

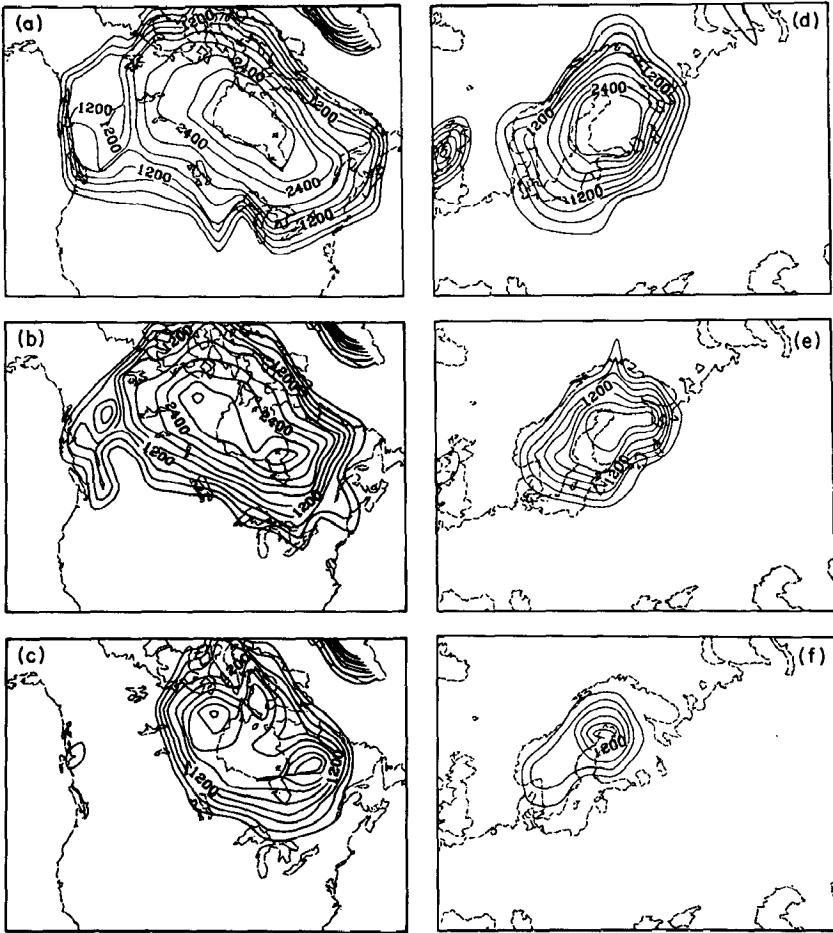


Figure 6 Plates (a), (b), and (c) show three time slices through the ICE-1 melting history at 18 KBP, 12 KBP, 8 KBP respectively for the North American ice complex. Plates (d), (e), (f) show the same sequence for Fennoscandia.

$\Delta R(\theta, \lambda, t)$, there is a severe problem involved in implementing (14) which has to do with M . This surface mass load functional may be expanded as

$$M = \rho_I L_I(\theta, \lambda, t) + \rho_w L_w(\theta, \lambda, t), \quad (15)$$

where ρ_I and ρ_w are the densities of ice and water respectively and where L_I and L_w are the corresponding thicknesses. The point to note here is that the functional M consists not only of the detailed ice history which we may estimate directly, but also of the water load in the ocean basins produced by the melting ice. Since we may safely assume the hydrological

cycle to be closed, mass conservation demands

$$\int d\Omega \rho_w L_w = M_w = - \int d\Omega \rho_I L_I = M_I \quad (16)$$

which is an integral constraint upon the load history. Given $M_I(t)$, the time-dependent mass flux to the oceans (assumed negative for melting), we can convert the corresponding M_w to a uniform equivalent time-dependent rise of *mean* sea level which we call

$$S_{\text{EUS}}(t) = \frac{M_w(t)}{\rho_w A_0} \quad (17)$$

where A_0 is the surface area of the Earth's oceans. $S_{\text{EUS}}(t)$, the so-called eustatic water rise, for the Peltier & Andrews history, agrees with the eustatic curve suggested by Shepard (1963) based upon the submergence curve for the Gulf of Mexico. This curve is clearly supposed to represent the average increase in water thickness over the ocean basins. If the actual rise of sea level locally were everywhere equal to this average, then L_w in (15) would be known from L_I and the convolution integral (14) could be evaluated. In fact, L_w is not everywhere constant and this poses the severe problem mentioned above. That L_w cannot increase uniformly over the ocean basins follows from the fact that if it did then the surface of the ocean would not remain equipotential during and after the deglaciation event. However, any deviation of the surface away from equipotential would set up currents in the ocean, which would redistribute water in such a way that this surface condition was restored. In order to predict relative sea level variations accurately, we must determine *where* in the oceans the meltwater actually goes. It turns out to be possible to answer this question rather accurately when a slightly more abstract view of sea level history is adopted, and this subject will be discussed in the next section.

RELATIVE SEA LEVELS

In order to satisfy the constraint that the surface of the oceans remain equipotential, we are obliged to consider the perturbations of potential associated with an arbitrary history of loading. These perturbations may clearly be calculated by convolving the load with the appropriate Green's function, which in this case is the third of those listed in (13). Let us suppose that the major ice sheets all melted at a single instant $t = 0$ so that the change of potential at $r = a$ may be computed as

$$\Delta\phi(\theta, \lambda, t) = \rho_I \phi_I^H * L_I + \rho_w \phi_w^H * S \quad (18)$$

where (\mathbf{I}^*) and (\mathbf{w}^*) represent convolutions over the ice and water respectively and where we have replaced L_w by S for later convenience. Now the change in potential $\Delta\phi$ will itself cause a change in sea level S , which is such as to ensure that the surface of the new ocean remains equipotential. This adjustment of sea level is in the amount (Farrell & Clark 1976, Peltier et al 1978)

$$S = \frac{\Delta\phi(\theta, \lambda, t)}{g} + C \quad (19)$$

where the constant C is fixed by the requirement of mass conservation. Equation (19) is a result from first-order perturbation theory and is therefore valid only for sufficiently small variations of bathymetry. From the manner in which it has been constructed, S is the local variation of sea level with respect to the solid surface of the planet and is therefore precisely the sea level history recorded in raised beaches such as the sequence shown in Figure 1. Substituting (19) into (18) we obtain

$$S = \rho_I \frac{\phi^H}{g} \mathbf{I}^* L_I + \rho_w \frac{\phi^H}{g} \mathbf{w}^* S + C. \quad (20)$$

An explicit expression for C is obtained by multiplying (20) by ρ_w and integrating over the surface area of the oceans; solving for C then gives

$$C = \frac{-M_I(t)}{\rho_w A_o} - \frac{1}{A_o} \left\langle \mathbf{I} \frac{\phi^H}{g} \mathbf{I}^* L_I + \rho_w \frac{\phi^H}{g} \mathbf{w}^* S \right\rangle_o, \quad (21)$$

since $-M_I(t) = \langle \rho_w S \rangle_o$ is the known mass loss history for the ice sheets in which $\langle \rangle_o$ indicates integration over the oceans.

With C given by (21), Equation (20) now constitutes an integral equation for S which we have called the sea level equation. Since it is an integral equation, with the unknown $S(\theta, \lambda, t)$ both on the left-hand side and under the convolution integral on the right, it must be solved using a matrix method. What we do is to divide the "active" area of the surface of the Earth (ice plus ocean) into a number of finite elements. The system is also discretized in time and to date we have elected to sample the S -history at equispaced intervals of 10^3 years, which is the same sampling interval employed to describe the input deglaciation model L_I . We assume that the mass load upon the finite element with centroid at \mathbf{r}' may be described by

$$L(\mathbf{r}', t) = \sum_{l=1}^P L_l(\mathbf{r}') H(t - t_l) \quad (22)$$

where the $t_i (i = 1, P)$ are a series of times that span the deformation history and the L_i are the loads applied or removed at the discrete times t_i . A complete description of the numerical methods employed for the solution of the general form of (20) will be found in Peltier et al (1978) and we will not repeat the detailed discussion here. Experience with the gravitationally self-consistent model embodied in (20) has shown that in the near field of the ice sheets the differences between its predictions and those based upon the assumption that the relative sea level history is essentially a measure of the local change in radius corrected by the eustatic sea level rise (e.g. Peltier & Andrews 1976) are small. The reason why these errors might be small is provided in Peltier (1980a) although it took explicit calculation to establish the fact.

Inspection of a sample solution to (20) shows that the rise of sea level in the ocean basins at points distant from the ice is quite nonuniform, with the greatest variation away from the 76.6 meter present-day average of ICE-1 being confined to the region nearest the ice. This may be taken as rather strong evidence to the effect that the notion of a eustatic rise of sea level should be used cautiously. By piercing such theoretically predicted global histories at longitude-latitude coordinates for which C^{14} data on relative sea level history exists, we may extract a specific prediction to compare with observations. Such predictions, as mentioned above, are dependent upon two unknown functionals of the model, namely, the viscosity profile of the Earth's interior and the assumed disintegration history. It is our ability to perform an initial linearization of the problem using a priori knowledge of the melting history that makes it possible to proceed. We first fix the ice history and determine a best $v(r)$. We then fix $v(r)$ and refine $L_i(\theta, \phi, t)$, continuing the iterative process until convergence is achieved. This procedure is precisely analogous to the use of free oscillation data to simultaneously constrain the interior elastic structure and the seismic moment tensor (Gilbert & Dziewonski 1975).

The first step along the iterative path was made by Peltier & Andrews (1976) who calculated sea levels using the approximate formula (14) in which ocean loading effects were neglected entirely, although a single calculation was shown, which suggested that these effects were weak in the near field of the ice, as mentioned above. Their conclusion from these initial calculations was that a model with uniform mantle viscosity was preferred. This conclusion was based almost entirely upon the fact that the model with high viscosity in the lower mantle predicted present-day rates of emergence in the central region that were much higher than observed. Very little data from the peripheral region had been compiled at that time and the model fit the far field data poorly because of the neglect of ocean

loading. Under the ice sheets the fit to the data was quite good when the uniform mantle viscosity model was employed.

A second step in this analysis was made in the papers by Clark et al (1978) and Peltier et al (1978) in which the gravitationally self-consistent model was first introduced. These calculations focused upon the ability of this general model to make accurate predictions at sites arbitrarily distant from the ice sheets. Use of the Peltier & Andrews load history showed that the predictions for the far field sites were time shifted from the observations such as to imply that melting should be delayed by about 2×10^3 years from the timing assumed by Peltier & Andrews. This time shift was therefore introduced and the far field data were fit rather accurately in consequence. This forward shift in timing of the disintegration, of course, had a disastrous effect upon the fits to the data at sites near the ice sheets; in particular, misfits to the emergence-submergence curves exceeded 300% at sites along the eastern seaboard of North America and at locations that were once under the Laurentide ice sheet (Peltier 1980a). We currently refer to the shifted version of the Peltier & Andrews melting history as ICE-2.

Given that the delayed melting characteristic of ICE-2 seemed required to fit the far field emergence data, the third step in the iterative process of refinement was to attempt to improve the agreement between theory and observation in the near field of the Laurentide ice sheet. The obvious way of effecting the desired reconciliation was to reduce the ice sheet thickness (Peltier et al 1978), since only in its vicinity were the misfits significant, and under the ice the errors were such that excessive emergence was predicted. The approach that we adopted (Wu & Peltier 1981b) was simply to reduce the thickness of Laurentide ice by the amount required to give the observed emergence of the 6 KBP beach at sites under the ice. This thickness correction was therefore a strong function of location (though a weak function of the viscosity model) and when it was applied led to an ice sheet with a much more irregular topography than that of the Peltier & Andrews model (ICE-1). This new ice history (to which we shall refer as ICE-3) was found to provide a good fit to the r.s.l. observations not only at sites under the ice sheet (which cannot be considered surprising) but also at sites in the peripheral region along the eastern seaboard of North America where the previous misfits had been enormous (Peltier et al 1978). As described by Wu & Peltier (1981b), with this new melting history the model exhibits some preference for an increase of viscosity with depth, and if a single step increase of viscosity is introduced at the seismic discontinuity at 670 km, then some of the sea level data prefer a lower mantle viscosity of about 10^{23} Poise. Values of lower mantle viscosity that are significantly

greater than this degrade the fit to the data, and not all data demand such an increase.

The basis of these statements is illustrated in Figure 7, where we show the observed r.s.l. histories at six sites, compared with the corresponding theoretical predictions from three viscosity models, which differ from one another only in the magnitude of the viscosity in the lower mantle below the 670 km discontinuity. The first three sites labelled (a), (b), (c) are, respectively, for Churchill, the Ottawa Islands, and Cape Henrietta Maria, all of which were located under the Laurentide ice sheet around Hudson Bay. Inspection of these emergence curves shows that they are not extremely sensitive to a modest increase of lower mantle viscosity although the model with a lower mantle viscosity of 5×10^{23} Poise is firmly rejected by all three data sets. Both the Churchill and Ottawa Islands sites prefer the uniform viscosity model and this preference is strongest at Ottawa Islands where the 10^{23} Poise lower mantle model predicts both too little net emergence and too high a present-day emergence rate [in accord with the previous conclusions of Peltier & Andrews (1976)]. At Churchill the amount of emergence is best fit by the uniform model, while the present-day emergence rate is best fit by the model with the 10^{23} Poise lower mantle. At Cape Henrietta Maria the model with the 10^{23} Poise lower mantle fits both characteristics best.

Plates (d), (e), and (f) of Figure 7 show the emergence data for Boston, Clinton, Connecticut, and Bermuda, respectively, all of which are located beyond the ice margin and at successively greater distances from the ice sheet center. The non-monotonic sea level history at Boston is characteristic of sites through which the peripheral bulge propagates, an effect which seems to be inhibited by high lower mantle viscosity (Peltier 1974). These data, therefore, prefer the uniform viscosity model. At both Clinton, Connecticut, and Bermuda, which are located at greater distance from the ice margin, the situation is reversed since at these locations the uniform model predicts too much submergence. Again, the model with the 5×10^{23} Poise lower mantle is nowhere preferred and so, to the extent that the ICE-3 load history is reasonable, this number is established as a firm upper bound on the viscosity of the lower mantle insofar as the relative sea level data are concerned.

The ICE-3 load history is, however, deficient from several points of view. Since melting is delayed by 2,000 years compared to the Peltier & Andrews history ICE-1, and since the locations of the terminal moraines in ICE-1 were controlled by data, it follows that the disintegration isochrones for ICE-3 may significantly violate the observational constraints. An equally serious criticism of ICE-3 is that it does not contain sufficient ice to explain the observed submergence in the far field (e.g. the r.s.l. curve

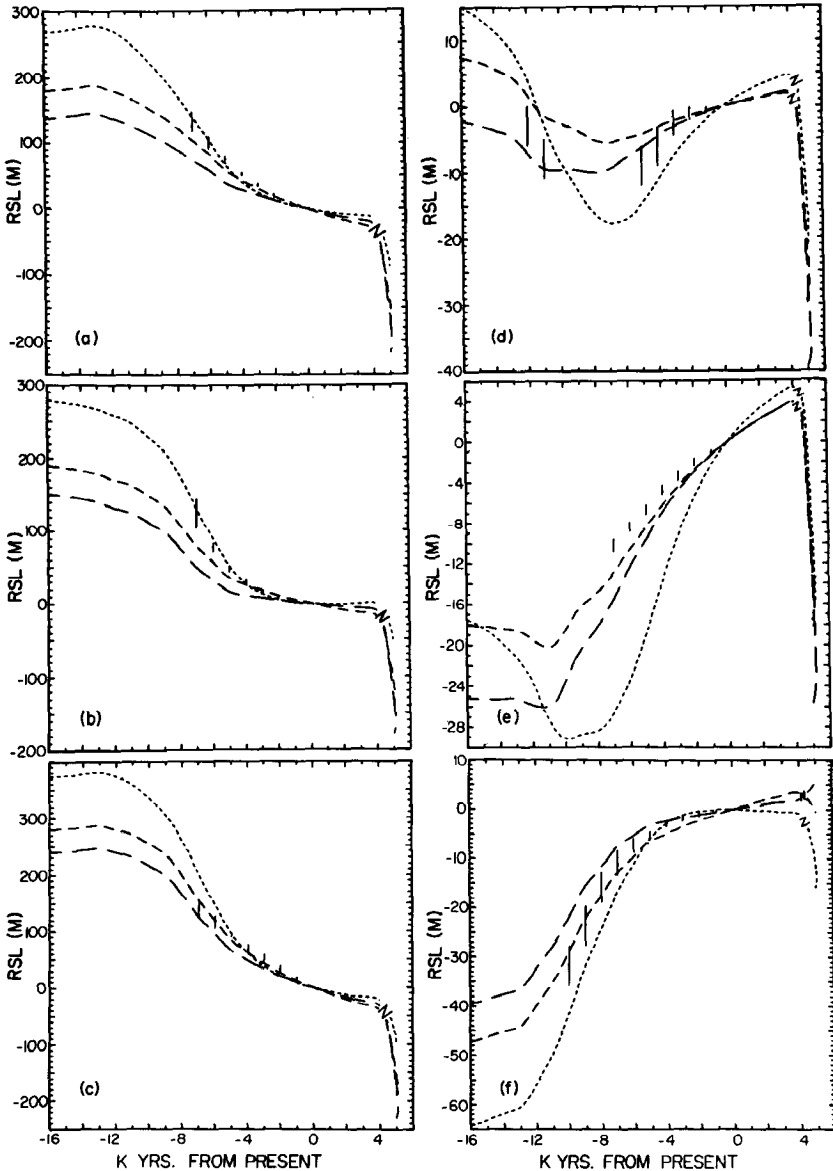


Figure 7 RSL histories at (a) Churchill, (b) Ottawa Islands, (c) Cape Henrietta Maria, (d) Boston, (e) Clinton, Connecticut, (f) Bermuda. The observed data with attached error bars are compared with predictions from three Earth models which differ from others only in the value of the mantle viscosity beneath a depth of 670 km. The short, intermediate, and long dashed curves are, respectively, for the model with lower mantle viscosity of 10^{23} Poise, with constant viscosity of 10^{22} Poise, and with lower mantle viscosity of 5×10^{23} Poise. The final dramatic excursion of each r.s.l. prediction ends at the point corresponding to the total r.s.l. variation that would be achieved in infinite time. The abscissa of this point is just the amount of emergence (submergence) remaining. The actual curves are, of course, discontinuous between the last two points since these should be separated by infinite time.

for the Gulf of Mexico). Although it may be possible to remedy this defect by melting an amount of ice equivalent to a eustatic rise of 15–20 meters from West Antarctica, it is not yet clear that this will not produce a significant (and perhaps adverse) effect on the northern hemisphere r.s.l. histories.

This brief discussion of the sea level data suffices to demonstrate that the inference of mantle viscosity from them is conditioned in a non-negligible way by the ice sheet history that one employs to make the predictions. Before we may be confident of the inferred viscosity we are obliged to investigate its sensitivity to plausible variations in the deglaciation model. As it happens [see Wu & Peltier (1981b) for details] the ICE-1 history with constant mantle viscosity also produces quite good fits to the r.s.l. curves at most near field sites and firmly rejects the model in which the lower mantle viscosity is 5×10^{23} Poise. In the next section, we investigate the extent to which free-air gravity data are able to provide confirmation of this inference from the r.s.l. information.

THE FREE-AIR GRAVITY ANOMALY

For a given viscoelastic Earth model and deglaciation history, solution of the sea level equation (20) yields a complete record of the loading of the ocean basins. Convolution of the ocean and ice loads with the Green's function for the free-air anomaly (13b) then provides a prediction of the free-air signal on the Earth's surface as

$$\Delta g(\theta, \lambda, t) = \Delta g'(\theta, \lambda, t) - \Delta g'(\theta, \lambda, \infty) \quad (23)$$

where

$$\Delta g'(\theta, \lambda, t) = \iint d\Omega' \int_0^t dt' \alpha(\theta|\theta', \lambda|\lambda', t|t') M(\theta', \lambda', t')$$

This form ensures that the free-air anomaly vanishes in the isostatic equilibrium configuration that obtains at infinite time. The free-air anomaly is a measure of the extent of isostatic disequilibrium. Clearly the calculation of $\Delta g(\theta, \lambda, \infty)$ requires the infinite-time Green's function $\alpha(\theta, \infty)$, the Heaviside form for which may be obtained from $\lim_{t \rightarrow \infty}$ of (13b). In this limit the Love numbers have the forms (12) and so correspond to the small s asymptotes of the spectra shown in Figure 3. It might be thought that one could compute the required $\alpha(\theta, \infty)$ simply by direct calculation of the Love numbers for sufficiently small s , but this turns out to be impossible since as $s \rightarrow 0$ the system (6) becomes "stiff" as its

order degenerates from sixth to second. As explained in Wu & Peltier (1981a), the required function $\alpha(\theta, \infty)$ must be calculated from Love numbers determined by solution of the degenerate second-order system. Our first attempt to calculate a free-air map (Peltier 1980b) was somewhat in error because of the failure to recognize this problem.

In Figure 8 we show the observed free-air gravity map for the Laurentide region (Walcott 1970). If one compares this anomaly with the ice sheet topography shown in Figure 6a, it is clear that both have the same elliptical form and that the minimum in the free-air map is coincident with the maximum of the ice sheet topography. The minimum value of the observed anomaly is approximately -35 milligals. In Figure 9 are shown six computed present-day free-air anomaly maps, three for each of the deglaciation models ICE-1 and ICE-3. The three calculations for each of the two ice histories are for the same three viscosity models as were employed in the previous discussion of relative sea levels.

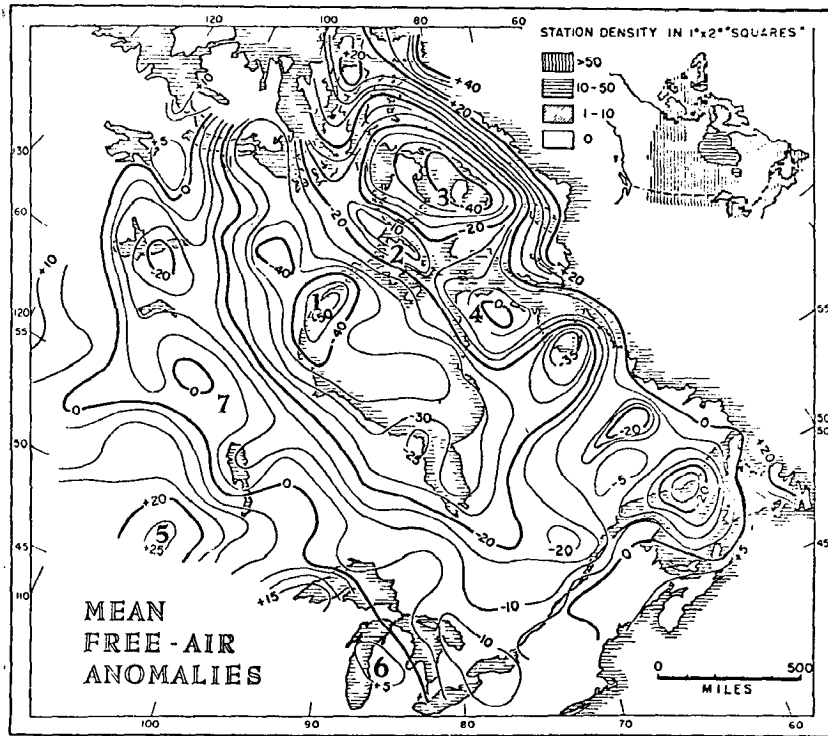


Figure 8 Free-air gravity anomaly map for the Laurentide region. Figure is from Walcott (1970).

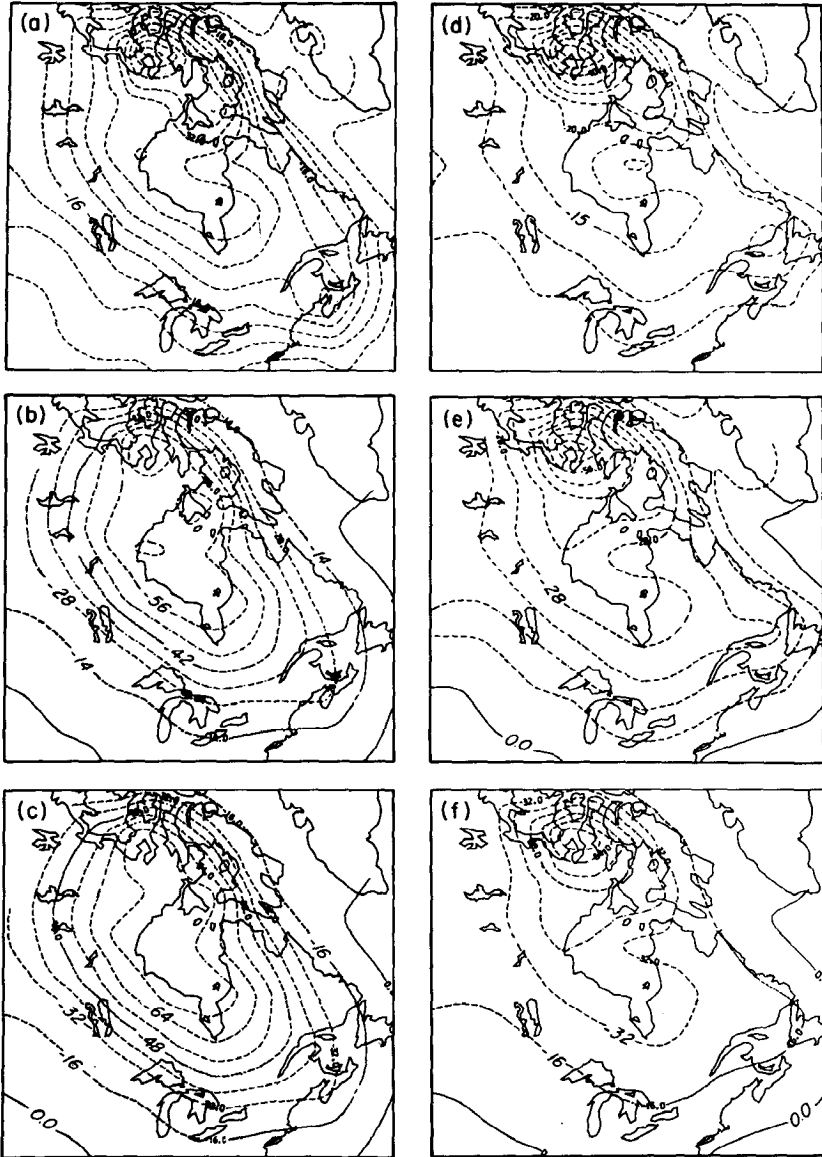


Figure 9 Free-air gravity predictions for the Laurentide region. Plates (a), (b), (c) show results from calculations based upon ICE-1 for the uniform viscosity model, that with a lower mantle viscosity of 10^{23} Poise, and that with a lower mantle viscosity of 5×10^{23} Poise. Plates (d), (e), and (f) show the same sequence of calculations but based upon the ICE-3 disintegration history.

Inspection of plates (a), (b), and (c), which correspond to the Peltier & Andrews history ICE-1, shows that the uniform viscosity model (plate a) gives a gravity anomaly very near that which is observed. Increasing the viscosity in the lower mantle (below the 670 km transition) from 10^{22} Poise to 10^{23} Poise [plate (b)] leads to a maximum anomaly in the central region on the order of 60 milligals, which is so much in excess of the observation that this model must be completely ruled out. The problem is only amplified when the lower mantle viscosity is further increased to 5×10^{23} Poise [plate (c)] since the maximum negative anomaly then increases to approximately 75 milligals. If the ICE-1 model were correct then the uniform viscosity mantle would be strongly preferred by the data as previously argued by Peltier & Andrews (1976) using only the r.s.l. information. However, as pointed out in the last section, ICE-1 cannot fit the far field emergence data, which seem to require that melting be delayed somewhat from the timing in ICE-1. With this delayed timing, the ice sheet thickness must be reduced in order to fit the sea level data and this new history (called ICE-3) was employed in the last section in demonstrating the ability of the model to fit the r.s.l. observations.

Plates (d), (e), and (f) of Figure 9 show the gravity anomaly for ICE-3 for the three mantle viscosity models. Plate (d) for the model with a uniform mantle viscosity of 10^{22} Poise shows that the maximum negative anomaly over Hudson Bay is significantly less than the observed (~ 20 mgals rather than ~ 35 mgals). Increasing the viscosity of the lower mantle to 10^{23} Poise [plate (e)] increases this anomaly to about 33 mgals, which is near the observed magnitude. A further increase of the viscosity of the lower mantle to 5×10^{23} Poise [plate (f)] leaves a present-day anomaly on the order of 38 mgals, which is somewhat larger than observed.

This sequence of comparisons very clearly demonstrates the extent to which the inference of the viscosity of the lower mantle is influenced by the assumed ice sheet melting history. For the thick ice sheet model that melts early (ICE-1), the uniform viscosity mantle is strongly preferred. For the thin ice sheet that melts late (ICE-3), an increase of the viscosity of the lower mantle is required to fit the observed free-air gravity anomaly but the lower mantle value cannot exceed about 10^{23} Poise, otherwise neither the gravity anomaly [plate (f)] nor the r.s.l. data (Figure 7) can be reconciled. The model with a lower mantle viscosity of 5×10^{23} Poise is rejected irrespective of the ice sheet history.

We consider the deglaciation histories ICE-1 and ICE-3 to be bounds upon the actual surface mass load functional. ICE-1, although it contains sufficient ice to explain the net submergence observed at far field sites (e.g. Gulf of Mexico) of about 80 meters, cannot explain the time (~ 6 KBP) at which raised beaches first appear along distant continental coastlines (e.g.

Reciffe, Brazil; New Zealand; Islands in the Indian Ocean) due to the tilting forced by the offshore water load. ICE-3, on the other hand, contains too little ice to explain the net emergence of raised beaches along distant continental coastlines at 6 KBP. It may be possible to remedy the mass defect of ICE-3 by introducing a substantial melting event in West Antarctic, but it remains to be demonstrated that such a melting event will not severely impact upon the northern hemisphere r.s.l. data. ICE-3, however, suffers from the additional defect that its disintegration isochrones do not match the observations (Prest 1969). The correct melting history is probably intermediate between ICE-1 and ICE-3 and therefore the viscosity of the lower mantle is probably intermediate between the values inferred with these two melting chronologies. This argument implies that an *upper* bound upon the viscosity of the mantle beneath the 670 km seismic discontinuity is 10^{23} Poise. A more detailed discussion of these ideas will be found in Wu & Peltier (1981b).

All of the discussion of gravity anomalies given here has been based upon the assumption that the planet and its ice sheets were in isostatic equilibrium at Wisconsin maximum. To the extent that isostatic equilibrium was not complete at that time, this initial disequilibrium will also impact upon the inference of mantle viscosity from the uplift data. Although, as discussed in Wu & Peltier (1981a), this effect should not be too severe, it might lead to the requirement for somewhat higher lower mantle viscosities than those mentioned above.

SUMMARY

The discussion in the previous sections of this article has illustrated several ways in which the planet has conspired to remember its response to the last deglaciation event of the current ice age. Each of these different modes of memory contributes a significant constraint upon the viscosity of the planetary mantle, and, in fact, provides information that is highly complementary rather than redundant. In order to simultaneously fit the relative sea level and free-air gravity data over Wisconsin Laurentia, the viscosity of the lower mantle is strongly restricted to be significantly less than 5×10^{23} Poise. The preferred value is a function of the unloading history assumed. If the Peltier & Andrews (1976) ICE-1 history is employed, then the preferred value of the viscosity of the lower mantle is the same as that of the upper, i.e. $\sim 10^{22}$ Poise. However, if the ICE-3 model is used, then some increase of viscosity in the lower mantle is necessary and a value in the neighborhood of 10^{23} Poise reconciles both data sets nicely. Neither the ICE-1 nor the ICE-3 loading histories are acceptable from all points of view. Melting occurs too early in ICE-1, as is evident from far field emer-

gence curves. On the other hand, melting is so much delayed in ICE-3 that its thickness must be reduced substantially in order to fit the near field r.s.l. data. This leads to the failure of ICE-3 to deliver sufficient water to the oceans to account for the observed net submergence (e.g. in the Gulf of Mexico). ICE-3 also violates the observed isochrones for the disintegration of the Laurentide sheet, which suggest a somewhat earlier retreat. It seems clear, therefore, that the ICE-1 and ICE-3 models are bounds upon the actual disintegration history and that the estimates of lower mantle viscosity which one obtains by employing them in the solution of the direct problem are themselves bounds upon the actual lower mantle viscosity. This leads to the conclusion that a value near 10^{23} Poise is the *upper* bound on the viscosity of the lower mantle beneath the seismic discontinuity at 670 km depth. This conclusion, it will be recalled from the introduction, is quite different from that of Walcott (1973) who believed that this value represented a *lower* bound upon the viscosity in this region. However, the conclusion is also different from that stated in Peltier & Andrews (1976) who, using the ICE-1 history, concluded that the lower mantle viscosity could not be significantly in excess of the upper mantle value of 10^{22} Poise. This conclusion is only valid to the extent that ICE-1 is valid and this model possesses the flaws mentioned above. Likewise, our conclusion contradicts that reached by Cathles (1975, 1980) who employed an ice sheet model for the Laurentide that was most like ICE-3, in that it was based upon the melting chronology of Bryson et al (1969) rather than the better controlled, and therefore more likely reliable, chronology of Prest (1969), which we used as the basis for ICE-1. Cathles' Laurentide model is thinner than ICE-1 and melting is delayed. Our analysis clearly shows that such a melting history will require an increase of lower mantle viscosity in order to explain the observed free-air gravity anomaly. Cathles did not employ these data to constrain his model and this led him to reach an overly strong conclusion regarding the value of the viscosity in the deep mantle.

One further implication of the results of the postglacial rebound analyses discussed here concerns the question of the depth extent of the convective circulation in the mantle which we suppose is responsible for driving the surface plates in the course of their relative motion. It has often been assumed in the past, on the basis of arguments to the effect that the viscosity of the deep mantle is extremely high, that convection must be confined to the upper mantle. The results presented here and discussed in detail in Wu & Peltier (1981a,b) show that this argument is untenable. If convection is confined to the upper mantle, confinement must be accomplished by some mechanism other than through a large increase of viscosity across the 670 km seismic discontinuity. In order to continue to support this

hypothesis, one is more or less obliged to invoke the existence of a marked change of mean atomic weight (i.e. chemistry) at this depth. As argued in Peltier (1973, 1980b), Jarvis & Peltier (1980a,b), Yuen & Peltier (1980a,b), Yuen et al (1980), and as assumed in the recent thermal history models of Sharpe & Peltier (1978, 1979), an equally plausible assumption is that the whole mantle is involved in the convective circulation. This model fits the surface observations very well and does so with a minimum of complexity. Its viability is strongly reinforced through interpretation of the observed geodynamic response to the current ice age.

ACKNOWLEDGMENTS

I have enjoyed profitable discussions with many colleagues concerning the subject matter of this paper, most recently with Patrick Wu, David Yuen, and Gary Jarvis, but initially also with Bill Farrell, Jim Clark, and John Andrews. I am indebted to all of them for useful observations and helpful suggestions. My research at the University of Toronto is sponsored by NSERCC grant A-9627. Several of the numerical computations discussed here were done on the CRAY-1 computer at the National Center for Atmospheric Research, which is sponsored by the National Science Foundation, and I am particularly indebted to Patrick Wu for his assistance with this phase of the work.

Literature Cited

- Anderson, D. L., Minster, J. B. 1979. The frequency dependence of Q in the Earth and implications for mantle rheology and Chandler wobble. *Geophys. J. R. Astron. Soc.* 58:431-40
- Andrews, J. T., Barry, R. G. 1978. Glacial inception and disintegration during the last glaciation. *Ann. Rev. Earth Planet. Sci.* 6:205-28
- Ballung, N. 1980. The land uplift in Fennoscandia, gravity field anomalies and isostasy. In *Earth Rheology Isostasy and Eustasy*, ed. N. A. Morner, pp. 297-321. Chichester: Wiley. 599 pp.
- Broecker, W. S., Van Donk, J. 1970. Insolation changes, ice volumes, and the O^{18} record in deep-sea cores. *Rev. Geophys.* 8:169-98
- Bryson, R. A., Wendland, W. M., Ives, J. D., Andrews, J. T. 1969. Radiocarbon isochrones on the disintegration of the Laurentide ice sheet. *Arctic Alp Res.* 1:1-13
- Buland, R., Gilbert, F. 1978. Improved resolution of complex eigenfrequencies in analytically continued seismic spectra. *Geophys. J. R. Astron. Soc.* 52:457-70
- Cathles, L. M. 1975. *The Viscosity of the Earth's Mantle*. Princeton Univ. Press. 386 pp.
- Cathles, L. M. 1980. Interpretation of post-glacial isostatic adjustment phenomena in terms of mantle rheology. In *Earth Rheology Isostasy and Eustasy*, ed. N. R. Morner, pp. 11-43. Chichester: Wiley. 599 pp.
- Clark, J. A., Farrell, W. E., Peltier, W. R. 1978. Global changes in postglacial sea level: a numerical calculation. *Quat. Res.* 9:265-87
- Daley, R. A. 1934. *The Changing World of the Ice Age*. Yale Univ. Press. 271 pp.
- Farrell, W. E. 1972. Deformation of the Earth by surface loads. *Rev. Geophys. Space Phys.* 10:761-97
- Farrell, W. E., Clark, J. A. 1976. On post-glacial sea level. *Geophys. J. R. Astron. Soc.* 46:647-67
- Gilbert, F., Dzierwonski, A. M. 1975. An application of normal mode theory to the retrieval of structural parameters and source mechanisms from seismic spectra. *Philos. Trans. R. Soc. London Ser. A* 278:187

- Jarvis, G. T., Peltier, W. R. 1980a. Ocean floor bathymetry profiles flattened by radiogenic heating in a convecting mantle. *Nature* 285(5767):649-51
- Jarvis, G. T., Peltier, W. R. 1980b. Mantle convection as a boundary layer phenomenon. *Geophys. J. R. Astron. Soc.* Submitted
- Jeffreys, H. 1973. Developments in geophysics. *Ann. Rev. Earth Planet. Sci.* 1:1-13
- Kohlstedt, D. L., Goetze, C. 1974. Low stress and high temperature creep in Olivine single crystals. *J. Geophys. Res.* 79:2045-51
- Liu, H. P., Anderson, D. L., Kanamorie, H. 1976. Velocity dispersion due to anelasticity: Implications for seismology and mantle composition. *Geophys. J. R. Astron. Soc.* 47:41-58
- McConnell, R. K. 1968. Viscosity of the mantle from relaxation time spectra of isostatic adjustment. *J. Geophys. Res.* 73:7089-7105
- Minster, J. B. 1980. Anelasticity and attenuation. In *Physics of the Earth's Interior*, ed. A. M. Dziewonski and E. Boschi. New York: Elsevier. In press
- Patterson, W. S. B. 1972. Laurentide ice sheet: Estimated volumes during late Wisconsin. *Rev. Geophys. Space Phys.* 10:885-917
- Peltier, W. R. 1973. Penetrative convection in the planetary mantle. *Geophys. Fluid Dynam.* 5:47-88
- Peltier, W. R. 1974. The impulse response of a Maxwell Earth. *Rev. Geophys. Space Phys.* 12:649-69
- Peltier, W. R. 1976. Glacial isostatic adjustment—II: The inverse problem. *Geophys. J. R. Astron. Soc.* 46:669-706
- Peltier, W. R. 1980a. Ice sheets, oceans, and the Earth's shape. In *Earth Rheology Isostasy and Eustasy*, ed. N. A. Morner, pp. 45-63. Chichester: Wiley. 599 pp.
- Peltier, W. R. 1980b. Mantle convection and viscosity. In *Physics of the Earth's Interior*, ed. A. M. Dziewonski and E. Boschi. New York: Elsevier
- Peltier, W. R. 1980c. Models of glacial isostasy and relative sea level. In *Dynamics of Plate Interiors*, ed. R. I. Walcott. Washington: AGU Publ.
- Peltier, W. R., Andrews, J. T. 1976. Glacial isostatic adjustment—I: The forward problem. *Geophys. J. R. Astron. Soc.* 46:605-46
- Peltier, W. R., Farrell, W. E., Clark, J. A. 1978. Glacial isostasy and relative sea level: a global finite element model. *Tectonophysics* 50:81-110
- Peltier, W. R., Yuen, D. A., Wu, P. 1980a. Postglacial rebound and transient rheology. *Geophys. Res. Lett.* 7(10):733-36
- Peltier, W. R., Wu, P., Yuen, D. A. 1980b. The viscosities of the Earth's mantle. In *Anelasticity of the Mantle*.
- Prest, V. K. 1969. Retreat of Wisconsin and Recent Ice in North America. *Geol. Surv. Can., Map 1257A*
- Sharpe, H. N., Peltier, W. R. 1978. Parameterized mantle convection and the Earth's thermal history. *Geophys. Res. Lett.* 5:737-44
- Sharpe, H. N., Peltier, W. R. 1979. A thermal history model for the Earth with parameterized convection. *Geophys. J. R. Astron. Soc.* 59:171-203
- Shepard, F. P. 1963. 35,000 years of sea level. In *Essays in Marine Geology*. Univ. Southern Calif. Press.
- Twiss, R. J. 1976. Structural superplastic creep and linear viscosity in the Earth's mantle. *Earth Planet. Sci. Lett.* 33:86-100
- Walcott, R. I. 1970. Isostatic response to loading of the crust in Canada. *Can. J. Earth Sci.* 7:716-27
- Walcott, R. I. 1973. Structure of the Earth from glacio-isostatic rebound. *Ann. Rev. Earth Planet. Sci.* 1:15-37
- Wu, P., Peltier, W. R. 1981a. Viscous gravitational relaxation. *Geophys. J. R. Astron. Soc.* Submitted
- Wu, P., Peltier, W. R. 1981b. The free air gravity anomaly as a constraint upon deep mantle viscosity. *Geophys. J. R. Astron. Soc.* Submitted
- Yuen, D., Peltier, W. R. 1980a. Mantle plumes and thermal stability of the D'' layer. *Geophys. Res. Lett.* 7(9):625-28
- Yuen, D., Peltier, W. R. 1980b. Temperature dependent viscosity and local instabilities in mantle convection. In *Physics of the Earth's Interior*, ed. A. M. Dziewonski and E. Boschi. New York: Elsevier.
- Yuen, D., Peltier, W. R., Schubert, G. 1980. On the existence of a second scale of convection in the upper mantle. *Geophys. J. R. Astron. Soc.* In press



CONTENTS

SOME REMINISCENCES OF ISOTOPES, GEOCHRONOLOGY, AND MASS SPECTROMETRY, <i>Alfred O. Nier</i>	1
PARTICLES ABOVE THE TROPOPAUSE: Measurements and Models of Stratospheric Aerosols, Meteoric Debris, Nacreous Clouds, and Noctilucent Clouds, <i>Owen B. Toon and Neil H. Farlow</i>	19
FORM, FUNCTION, AND ARCHITECTURE OF OSTRACODE SHELLS, <i>Richard H. Benson</i>	59
MECHANICS OF MOTION ON MAJOR FAULTS, <i>Gerald M. Mavko</i>	81
ROTATION AND PRECESSION OF COMETARY NUCLEI, <i>Z. Sekanina</i>	113
THE SIGNIFICANCE OF TERRESTRIAL ELECTRICAL CONDUCTIVITY VARIATIONS, <i>G. D. Garland</i>	147
METAMORPHOSED LAYERED IGNEOUS COMPLEXES IN ARCHEAN GRANULITE-GNEISS BELTS, <i>Brian F. Windley, Finley C. Bishop, and Joseph V. Smith</i>	175
ICE AGE GEODYNAMICS, <i>W. R. Peltier</i>	199
NUCLEATION AND GROWTH OF STRATOSPHERIC AEROSOLS, <i>A. W. Castleman, Jr., and Robert G. Keese</i>	227
ANCIENT MARINE PHOSPHORITES, <i>Richard P. Sheldon</i>	251
DEPLETED AND FERTILE MANTLE XENOLITHS FROM SOUTHERN AFRICAN KIMBERLITES, <i>P. H. Nixon, N. W. Rogers, I. L. Gibson, and A. Grey</i>	285
THE COMBINED USE OF OXYGEN AND RADIOGENIC ISOTOPES AS INDICATORS OF CRUSTAL CONTAMINATION, <i>David E. James</i>	311
INTERVALENCE TRANSITIONS IN MIXED-VALENCE MINERALS OF IRON AND TITANIUM, <i>Roger G. Burns</i>	345
FREE OSCILLATIONS OF THE EARTH, <i>Ray Buland</i>	385
LONG WAVELENGTH GRAVITY AND TOPOGRAPHY ANOMALIES, <i>A. B. Watts and S. F. Daly</i>	415
THE BIOGEOCHEMISTRY OF THE AIR-SEA INTERFACE, <i>Leonard W. Lion and James O. Leckie</i>	449
INDEXES	
Author Index	487
Cumulative Index of Contributing Authors, Volumes 5-9	498
Cumulative Index of Chapter Titles, Volumes 5-9	500